Transactions Papers

Achieving Near-Capacity Performance on Multiple-Antenna Channels with a Simple Concatenation Scheme

Nghi H. Tran, *Member, IEEE,* Tho Le-Ngoc, *Fellow, IEEE*, Tad Matsumoto, *Fellow, IEEE*, and Ha H. Nguyen, *Senior Member, IEEE*

***Abstract*—This paper proposes a capacity-approaching, yet simple scheme for multi-input multiple-output (MIMO) channels. The proposed scheme is based on a concatenation of a mixture of short memory-length convolutional codes or repetition codes and a short, and simple rate-1 linear block code, followed by either 1-dimensional (1-D) anti-Gray or Gray mapping of quadrature phase-shift keying (QPSK) modulation. By interpreting the rate-1 code and the 1-D mapping as a multi-D mapping performed over multiple transmit antennas, the error performance is analyzed in two regions. In the error-floor region, a tight union bound and the corresponding design criterion on the asymptotic performance are derived. The bound provides a useful tool to predict the error performance at relatively low bit error rate (BER) values. Based on the obtained design criterion, an optimal rate-1 code for each 1-D mapping is then constructed to achieve the best asymptotic performance. In the turbo pinch-off region, by using extrinsic information transfer (EXIT) charts, the most suitable mixed codes are selected for both symmetric and asymmetric antenna configurations. It is demonstrated that the simple concatenation scheme can achieve a near-capacity performance over the MIMO channels. Furthermore, its error performance is shown to be comparable to that obtained by using well-designed irregular LDPC and RA codes, and therefore, the proposed scheme significantly outperforms a scheme employing a parallel concatenated turbo code. Simulation results in various cases are provided to verify the analysis.**

***Index Terms*—Multiple-antenna channels, capacity-approaching performance, EXIT chart, convolutional code, repetition code, block code, anti-Gray mapping, Gray mapping, multi-dimensional mapping, error bound.**

Paper approved by T. M. Duman, the Editor for Coding Theory and Applications of the IEEE Communications Society. Manuscript received February 25, 2009; revised August 2, 2009.

N. H. Tran and T.-L. Ngoc are with the Department of Electrical & Computer Engineering, McGill University, Canada (e-mail: {nghi.tran, tho.le-ngoc}@mcgill.ca).

T. Mastumoto is with the Japan Advanced Institute of Science and Technology, Japan, and Center for Wireless Communication at the University of Oulu, Finland (e-mail: matumoto@jaist.ac.jp).

H. H. Nguyen is with the Department of Electrical & Computer Engineering, University of Saskatchewan, Canada (e-mail: ha.nguyen@usask.ca).

This work was supported in part by NSERC and by the Japanese government funding program, Grant-in-Aid for Scientific Research (B), No. 20360168. A part of this work was presented at the 6th ICST BROADNET Conference, Madrid, Spain Sept. 2009 and at the IEEE Globecom Conference, Hawaii, USA Dec. 2009.

Digital Object Identifier 10.1109/TCOMM.2010.04.090116

I. Introduction

It has been widely acknowledged that the use of multiple antennas at the transmitter and/or receiver provides a much higher channel capacity compared to that of single-antenna counterparts over wireless fading channels [1], [2]. With the recent developments in iterative decoding, a number of pragmatic approaches using powerful turbo-like codes such as low density parity check (LDPC) codes, repeat-accumulate (RA) codes, or turbo codes themselves have been proposed [3]–[6] to achieve a close-capacity performance under a bit-interleaved coded modulation (BICM) framework [7], [8]. For instance, by directly transmitting signals that are coded with an outer turbo code, it was shown in [3] that a near-capacity performance can be attained in a symmetric antenna setup where the number of receive antennas equals the number of transmit antennas. However, the error performance of such turbo-coded systems experiences a severe degradation when the antenna scenario is asymmetric [4], [9], i.e., the number of receive antennas is smaller than the number of transmit antennas. As an alternative, reference [4] proposes an LDPC coded modulation scheme that performs very close to the capacity limit, even when the antenna setup is asymmetric. Using a similar approach as in [4], equally good performances are also obtained in [5] by using outer irregular RA codes.

In the above-mentioned coded modulation methods employing either LDPC, RA, or turbo codes, the mapping function from binary bits to signal points is implemented independently and identically for each transmit antenna using complex 1-dimensional (1-D) Gray mapping. More recently, the idea of multi-D mapping, first proposed for single-antenna channels [10]–[12], has been further adopted in a multiple-antenna system together with an outer convolutional code [13]. In a multi-D mapping system, a group of binary bits is simultaneously mapped to multi-D signal points in such a way that a signal pair at a larger Euclidean distance corresponds to a smaller Hamming distance in labeling [11]. By considering only the symmetric antenna scenario, it was demonstrated in [13] that a significant coding gain can be achieved by using only a simple convolutional code. However, the simulation results in [13] indicate that the performance of a turbo coded

system employing conventional Gray mapping is still better than that of the multi-D mapping system. Furthermore, since [13] only considers the symmetric antenna setup, it is not clear how the multi-D mapping system performs in the asymmetric scenario. The advantage of a multi-D mapping system is that it offers a lower decoding complexity than a system using turbo-like codes, since only a soft-output decoder of a simple convolutional code is required. To our best knowledge, the designs in [4] using LDPC codes and in [5] with RA codes are still the most effective coded modulation techniques over multiple-antenna wireless fading channels under various antenna configurations.

This paper is also concerned with the multi-D mapping technique but in a different paradigm for near-capacity performance over both symmetric and asymmetric multiple-antenna channels with quadrature phase-shift keying (QPSK) modulation. In particular, a capacity-approaching but yet simple serial concatenation of a mixture of short memory-length convolutional codes or repetition codes and a short rate-1 linear block code followed by either 1-D anti-Gray or Gray mapping[1] is introduced. By interpreting rate-1 code together with the 1-D mapping as a multi-D mapping employed over multiple transmit antennas, the error performance is analyzed in two regions, the error-floor and turbo pinch-off regions. In the former one, a tight union bound and design criterion on the asymptotic performance are derived, which provide a useful mathematical tool to predict the error performance at relatively low bit error rate (BER). These derivations allow us to determine optimal rate-1 block codes for anti-Gray and Gray mappings to achieve the best asymptotic performance. The turbo pinch-off region is then examined using extrinsic information transfer (EXIT) chart [4], [14], [15] to identify the most suitable mixed code for each antenna configuration. It is demonstrated that the simple concatenation scheme achieves near-capacity performance. In some cases, the selected mixed code is just a simple repetition code. Furthermore, analytical and simulation results indicate that a comparable performance to that using well-designed irregular LDPC and RA codes in [4], [5] can be achieved. Its also means that the proposed scheme significantly outperforms a scheme employing a parallel concatenated (turbo) code, especially when there are more transmit antennas than receive antennas, while having a lower computational complexity. This novel, high-performance yet low-complexity scheme would therefore have potential applications in the next and future generations of wireless communications using multiple antennas.

The remaining of the paper is organized as follows. Section II introduces the system model. In Section III, the error analysis based on the assumption of perfect *a priori* information fed back from the decoder to the demodulator is derived. A design criterion on the asymptotic performance is also provided in this section. These derivations are helpful in predicting the BER performance and in constructing optimal rate-1 codes. Section IV studies the turbo pinch-off region for the system under consideration by using the EXIT chart technique. Comparison with schemes employing LDPC and RA codes proposed in [4], [5] is also made in this section. Numerical and simulation results are provided in Section V to demonstrate the advantages of the proposed system. Finally, Section VI concludes the paper.

It should be noted that this paper assumes an ergodic multiple-input multiple-output (MIMO) fading channel model where only the receiver but not the transmitter knows the channel. Furthermore, similar to [3], [4], a direct transmission over multiple transmit antennas is considered without the use of special multiple-antenna code-design such as space-time codes [16]–[19]. It is certainly absorbing to further extend the proposed technique to cover both spatial and temporal domains. The possibility of exploiting its advantage in adaptive coded-modulation where the channel knowledge is available at both the transmitter and receiver would also be of particular interest for further studies.

II. System Model

A. Transmitter

A block diagram of the transmitter of the proposed concatenation system equipped with N_t transmit and N_r receive antennas is depicted in Fig. 1 (a). First, a binary information block $\underline{\boldsymbol{u}}$ of length L_u is divided into two binary sequences $\underline{\boldsymbol{u}}_I$ and $\underline{\boldsymbol{u}}_{II}$ of lengths L_I and L_{II}, respectively, using a demultiplexer. Each sequence $\underline{\boldsymbol{u}}_l$, $l \in \{I, II\}$, is encoded by a suitable rate-k_l/n_l binary encoder C_l into a coded sequence $\underline{\boldsymbol{c}}_l$ consisting of $T_l = L_l n_l / k_l$ coded bits. These binary encoders could be simple convolutional or repetition codes and shall be determined later. Coded sequences $\underline{\boldsymbol{c}}_I$ and $\underline{\boldsymbol{c}}_{II}$ are then serially combined by a multiplexer to create a coded sequence $\underline{\boldsymbol{c}}$ of length $T_c = T_I + T_{II}$. This encoding structure, inherited from the code doping technique proposed in [20], [21], is referred to as a mixed code of $K = 2$ binary codes, with code doping ratio $\alpha = L_I/L_u$. The value of α is in the range $0 \le \alpha < 1$. For $\alpha = 0$, there is only a single code C_{II}, whilst for $0 < \alpha < 1$, a code C_I is added producing a mixed code. As shall be shown later, this mixed code provides a flexible structure to control the convergence behavior of the system. Note that the number of binary encoders can be straightforwardly generalized to $K > 2$. Furthermore, the use of a single outer convolutional or repetition code is a special case of the proposed mixed code for $\alpha = 0$.

After being interleaved, each group of $M = 2N_t$ coded bits of the interleaved sequence $\underline{\tilde{\boldsymbol{c}}}$, denoted as $\boldsymbol{v} = (v_1, v_2, \ldots, v_M)^\top$, is fed to a rate-1 linear block code with generator matrix $\boldsymbol{G}$ of size $M \times M$ over Galois field 2 (GF(2)). The design of $\boldsymbol{G}$ is discussed in the next section. A vector of M output coded bits $\boldsymbol{b} = (b_1, b_2, \ldots, b_M)^\top$ is given as:

$$\boldsymbol{b} = \boldsymbol{G} \cdot \boldsymbol{v}. \tag{1}$$

In (1), all operations are defined over GF(2). To guarantee that there is one-to-one correspondence between $\boldsymbol{v}$ and $\boldsymbol{b}$, a condition of invertibility is imposed on $\boldsymbol{G}$, i.e., $\boldsymbol{G}$ is a full-rank matrix. Then two consecutive bits (b_{2i-1}, b_{2i}), $1 \le i \le N_t$, are grouped together and mapped to a complex QPSK symbol s_i using either 1-D anti-Gray or Gray mapping. A sequence of N_t 1-D complex symbols $\{s_i\}$ is considered to be a super symbol $\boldsymbol{s} = [s_1, s_2, \ldots, s_{N_t}]^\top$ in an N_t-D constellation $\boldsymbol{\Psi}$

[1] Anti-Gray and Gray mappings are the only two mapping rules available for QPSK.

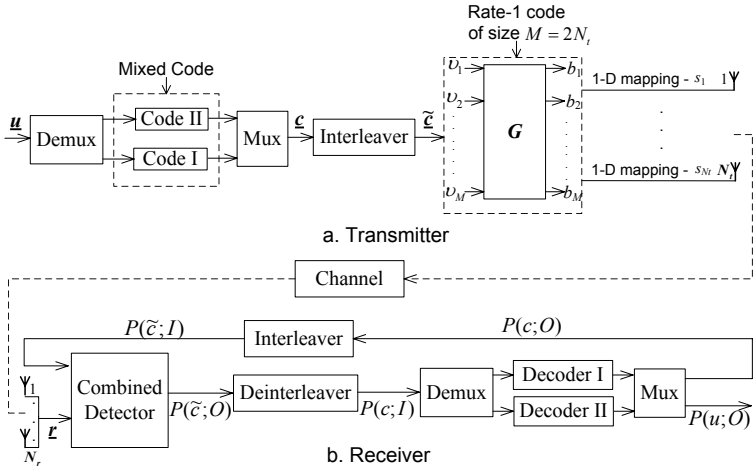

Fig. 1. The proposed concatenation scheme equipped with N_t transmit and N_r receive antennas.

with cardinality $|\mathbf{\Psi}| = 2^M$. Each component s_i is finally transmitted by the ith transmit antenna.

The combination of rate-1 block code and 1-D mapping above can be interpreted as a special case of a multi-D mapping technique in which a vector of M binary bits $\boldsymbol{v} = [v_1, v_2, \ldots, v_M]^\top$ are mapped directly to a super symbol $\boldsymbol{s}$ according to some multi-D mapping rule [11], [13]. Hereafter, vector $\boldsymbol{v}$ is referred to as the label of $\boldsymbol{s}$. Theoretically, there are $(2^M)!$ possible mappings for $\mathbf{\Psi}$. These mapping can be further classified in a smaller number of classes, each consisting of two or more mappings that result in an identical performance [22]. It is possible to find an equivalent rate-1 code for a certain class of mapping. However, this paper focuses only on optimal rate-1 codes in terms of the asymptotic performance. As we shall see shortly, given an outer mixed code, there exists an optimal rate-1 code for each 1-D mapping that yields the same optimal multi-D mapping ξ over all possible mappings of $\mathbf{\Psi}$, and hence achieves the best asymptotic performance.

B. Receiver

Consider an ergodic frequency-flat Rayleigh fading channel. The $N_r \times 1$ received vector $\boldsymbol{r}$ is given as:

$$\boldsymbol{r} = \boldsymbol{H} \cdot \boldsymbol{s} + \boldsymbol{n}. \tag{2}$$

In (2), the matrix $\boldsymbol{H}$ is an $N_r \times N_t$ complex matrix known perfectly at the receiver and its components are $\mathcal{CN}(0,1)$[2], $\boldsymbol{n}$ is an $N_r \times 1$ vector representing additive white Gaussian noise (AWGN) whose entries are $\mathcal{CN}(0, N_0)$.

At the receiver, a typical concatenation of a MIMO detector, an *a posteriori* probability (APP) bit decoder of the rate-1 block code, and a soft-input soft-output (SISO) outer decoder can be applied. Similar to the design in [5], the MIMO detector and rate-1 block decoder can be combined in one block as shown in Fig. 1 (b) to reduce decoding complexity and improve robustness. More specifically, by representing the rate-1 block code and 1-D mapping as a multi-D mapping ξ, the combined detector performs APP detection to provide the extrinsic probability of the k coded bit v_k, $1 \le k \le M$, being set at b, $b \in \{0,1\}$, as:

$$P(v_k = b; O) = \sum_{\boldsymbol{s} \in \mathbf{\Psi}_b^k} \left[\exp\left(-\frac{||\boldsymbol{r} - \boldsymbol{H} \cdot \boldsymbol{s}||^2}{N_0} \right) \prod_{j \neq k} P\left(v_j = v_j(\boldsymbol{s}); I\right) \right] \tag{3}$$

In (3), $\mathbf{\Psi}_b^k$ denotes a subset of $\mathbf{\Psi}$ that contains all symbols whose labels have the value b at the kth position. Clearly, $\mathbf{\Psi}_b^k$ is determined by the mapping rule ξ. Furthermore, $v_j(\boldsymbol{s})$ is the value of the jth bit in the label of $\boldsymbol{s}$ and $P\left(v_j = v_j(\boldsymbol{s}); I\right)$ is the *a priori* probability of the other bits, $j \neq k$, on the same channel symbol. Observe that the computation of the extrinsic information of the coded bit in (3) involves the set of 2^{M-1} super symbols in $\mathbf{\Psi}_b^k$, which has the same complexity as that of the MIMO detector [3], [4]. Note that, for a multi-D mapping system, it is not possible to apply some low-complexity demodulators, such as the SISO minimum mean squared error (MMSE) detectors proposed in [23], [24]. This is because all N_t transmit antennas are connected by the mapping and the demodulation process cannot be performed separately on each interfering $1 \times N_r$ subchannel. However, some other simple and suboptimal demodulation methods, such as the list sphere decoder in [3], can be used to reduce the complexity. Since this paper emphasizes on the near-capacity performance, only the APP detector shall be implemented.

Let $\{P(\tilde{c} = b; O)\}$ be the sequence of the extrinsic information of T coded bits at the output of the detector. As shown in Fig. 1 (b), its deinterleaved version is then demultiplexed and the extrinsic information of the corresponding T_I and T_{II} coded bits is forwarded to the two SISO channel decoders, respectively. For convolutional codes, the SISO channel decoder uses the forward-backward algorithm [25], [26]. If the binary encoder is a rate-$1/n$ repetition code, the extrinsic information for each coded bit is simply calculated as:

$$P(c_i = b; O) = \prod_{j=1, j \neq i}^{n} P\left(c_j = b; I\right). \tag{4}$$

There is an iterative processing between the combined detector and outer channel decoder to exchange the extrinsic informa-

[2]Here $\mathcal{CN}(0, \sigma^2)$ denotes a circularly symmetric complex Gaussian random variable with variance $\sigma^2/2$ per dimension.

tion of the coded bits $P(\tilde{c};O)$ and $P(c;O)$. After being interleaved, $P(\tilde{c};O)$ and $P(c;O)$ become the *a priori* information $P(c;I)$ and $P(\tilde{c};I)$ at the input of the SISO decoder and the combined detector, respectively. The *a posteriori* probabilities of the information bits can be computed to make the hard decisions at the output of the decoder after each iteration.

III. Tight Union Bound and Design Criterion on The Asymptotic Performance and Optimal Rate-1 Codes

With the representation of the rate-1 block code together with 1-D mapping as a multi-D mapping ξ, this section presents a tight union bound on the asymptotic performance of the proposed system. The derivation is based on the assumption of an ideal interleaver and perfect *a priori* information of coded bits fed back from the decoder to the combined detector as normally seen in the analysis of BICM with iterative decoding (BICM-ID) systems [11], [27]. The derived bound can be used to accurately predict the asymptotic BER performance without the need of time-consuming simulations. Furthermore, a design criterion is obtained, which is helpful in developing an optimal rate-1 code together with either anti-Gray or Gray mapping.

A. Tight Union Bound and Design Criterion on The Asymptotic Performance

Following the analysis in [8], the bit error probability (BEP) for a BICM system using a mixed code with code doping ratio α and an ideal interleaver can be expressed as:

$$P_b = \alpha P_b^{(I)} + (1-\alpha)P_b^{(II)}, \tag{5}$$

where $P_b^{(I)}$ and $P_b^{(II)}$ are the BEPs of BICM systems using binary codes I and II, respectively. When the lth component code is a rate-k_l/n_l convolutional code, the union bound on $P_b^{(l)}$ is expressed as [8]:

$$P_b^{(l)} \le \frac{1}{k_l}\sum_{d=d_H^{(l)}}^{\infty} c_d^{(l)} f(d,\mathbf{\Psi},\xi), \tag{6}$$

In (6), $c_d^{(l)}$ is the total information weight of all of the error events at Hamming distance d and $d_H^{(l)}$ is the free Hamming distance of the binary code l. In the case that the lth component code is a rate-k_l/n_l block code, the summation in (6) is taken from $d_H^{(l)}$ to n_l, since the Hamming distance between two codewords is less than or equal to n_l [8]. The function $f(d,\mathbf{\Psi},\xi)$ is an average pairwise error probability (PEP), which depends on the Hamming distance d, the constellation $\mathbf{\Psi}$, and the mapping rule ξ. In the following, the function $f(d,\mathbf{\Psi},\xi)$ is computed from the PEP of two codewords.

Let $\underline{\boldsymbol{c}}$ and $\breve{\underline{\boldsymbol{c}}}$ be the input and decoded sequences with Hamming distance d and without loss of generality, assume that they differ in the first d consecutive bits. With the use of a sufficiently long interleaver, it can be assumed that the binary sequences $\underline{\boldsymbol{c}}$ and $\breve{\underline{\boldsymbol{c}}}$ correspond to symbol sequences $\underline{\boldsymbol{S}}$ and $\breve{\underline{\boldsymbol{S}}}$ of d N_t-D signal points $\underline{\boldsymbol{S}} = [\boldsymbol{s}_1,\ldots,\boldsymbol{s}_d]$ and $\breve{\underline{\boldsymbol{S}}} = [\breve{\boldsymbol{s}}_1,\ldots,\breve{\boldsymbol{s}}_d]$. Here, $\boldsymbol{s}_e$ and $\breve{\boldsymbol{s}}_e$, $1 \le e \le d$, belong to the constellation $\mathbf{\Psi}$. Also, let $\underline{\boldsymbol{H}} = [\boldsymbol{H}_1,\ldots,\boldsymbol{H}_d]$ be the sequence of channel matrices. Similar to the analysis in [16], after averaging over the channel sequence $\underline{\boldsymbol{H}}$, the unconditional PEP between $\underline{\boldsymbol{S}}$ and $\breve{\underline{\boldsymbol{S}}}$ can be obtained by using the Gaussian probability integral $Q\left(\sqrt{2\gamma}\right) = \frac{1}{\pi}\int_0^{\pi/2}\exp\left(-\frac{\gamma}{\sin^2\theta}\right)\mathrm{d}\theta$ as:

$$P(\underline{\boldsymbol{S}} \to \breve{\underline{\boldsymbol{S}}}) = \frac{1}{\pi}\int_0^{\pi/2}\left(\prod_{e=1}^{d}\Delta_e\right)\mathrm{d}\theta, \tag{7}$$

where

$$\Delta_e = \prod_{i=1}^{N_t}\left(1+\frac{1}{4N_0}\frac{\lambda_{e,i}}{\sin^2\theta}\right)^{-N_r}. \tag{8}$$

In (8), $\{\lambda_{e,i}\}$ are the eigenvalues of $\boldsymbol{A}_e = (\boldsymbol{s}_e - \breve{\boldsymbol{s}}_e)(\boldsymbol{s}_e - \breve{\boldsymbol{s}}_e)\dagger$. Since $\boldsymbol{s}_e$ and $\breve{\boldsymbol{s}}_e$ are N_t-D vectors, Δ_e can be simplified to:

$$\Delta_e = \left(1+\frac{||\boldsymbol{s}_e - \breve{\boldsymbol{s}}_e||^2}{4N_0\sin^2\theta}\right)^{-N_r}. \tag{9}$$

With an assumption that perfect *a priori* information of coded bits fed back from the decoder to the combined detector is achieved, one has an ideal knowledge of the other coded bits carried by the transmitted symbol $\boldsymbol{s}_e$. As a result, only two signal points $\boldsymbol{s}_e$ and $\breve{\boldsymbol{s}}_e$ whose labels differ in only 1 bit need to be considered. Then the union bound on $f(d,\mathbf{\Psi},\xi)$ can be computed by averaging over all signal points $\boldsymbol{s}$ and $\boldsymbol{p}$ in the N_t-D constellation $\mathbf{\Psi}$ whose labels differ in only 1 bit at position k, $1 \le k \le M$ as

$$f(d,\mathbf{\Psi},\xi) \le \frac{1}{\pi}\int_0^{\pi/2} E\left\{\left(1+\frac{||\boldsymbol{s}-\boldsymbol{p}||^2}{4N_0\sin^2\theta}\right)^{-N_r}\right\}^d \mathrm{d}\theta, \tag{10}$$

where

$$\begin{aligned} & E\left\{\left(1+\frac{||\boldsymbol{s}-\boldsymbol{p}||^2}{4N_0\sin^2\theta}\right)^{-N_r}\right\} \\ = \; & \frac{1}{M2^M}\sum_{\boldsymbol{s}\in\mathbf{\Psi}}\sum_{k=1}^{M}\left[\left(1+\frac{||\boldsymbol{s}-\boldsymbol{p}||^2}{4N_0\sin^2\theta}\right)^{-N_r}\right]. \end{aligned} \tag{11}$$

The single integral in (10) can be efficiently computed and, as shall be verified later, it provides an accurate approximation on the BER performance in the error-floor area.

To understand the influence of a multi-D mapping ξ to the asymptotic behavior of the BER, one can apply the inequality $Q\left(\sqrt{2\gamma}\right) < \frac{1}{2}\exp(-\gamma)$. It is then easy to verify that the function $f(d,\mathbf{\Psi},\xi)$ can be approximated as:

$$f(d,\mathbf{\Psi},\xi) \sim \frac{1}{2}\left[\delta(\mathbf{\Psi},\xi)\right]^d, \tag{12}$$

where $\delta(\mathbf{\Psi},\xi)$ is written as:

$$\delta(\mathbf{\Psi},\xi) = \frac{1}{M2^M}\sum_{\boldsymbol{s}\in\mathbf{\Psi}}\sum_{k=1}^{M}\left[\left(1+\frac{||\boldsymbol{s}-\boldsymbol{p}||^2}{4N_0}\right)^{-N_r}\right]. \tag{13}$$

At high signal to noise ratio (SNR), $\delta(\mathbf{\Psi},\xi)$ can be further simplified to

$$\begin{aligned} \delta(\mathbf{\Psi},\xi) &\approx (4N_0)^{N_r}\left(\frac{1}{M2^M}\sum_{\boldsymbol{s}\in\mathbf{\Psi}}\sum_{k=1}^{M}||\boldsymbol{s}-\boldsymbol{p}||^{-2N_r}\right) \\ &= (4N_0)^{N_r}\hat{\delta}(\mathbf{\Psi},\xi). \end{aligned} \tag{14}$$

where

$$\hat{\delta}(\mathbf{\Psi},\xi)=\frac{1}{M2^M}\sum_{\boldsymbol{s}\in\mathbf{\Psi}}\sum_{k=1}^{M}||\boldsymbol{s}-\boldsymbol{p}||^{-2N_r}. \tag{15}$$

The parameter $\hat{\delta}(\mathbf{\Psi},\xi)$ above does not depend on SNR and it can be conveniently used to characterize the effect of a mapping ξ to the asymptotic performance. More specifically, in terms of the asymptotic performance, $\hat{\delta}(\mathbf{\Psi},\xi)$ should be made as small as possible to minimize the BER. Loosely speaking, this can be done by using a mapping rule ξ such that two signal points $\boldsymbol{s}$ and $\boldsymbol{p}$ whose labels differ in only 1 bit should be placed as far apart as possible in terms of the Euclidean distance. In the next subsection, in combining with either anti-Gray or Gray mapping, an optimal rate-1 code is introduced to minimize $\hat{\delta}(\mathbf{\Psi},\xi)$ in (15) over all mapping rules $\{\xi\}$ of $\mathbf{\Psi}$.

B. Optimal Rate-1 Block Codes

Without loss of generality, assume that the coordinates of the four QPSK symbols are $[+1,+1]$, $[+1,-1]$, $[-1,+1]$, and $[-1,-1]$. By representing the super constellation $\mathbf{\Psi}$ as a hypercube in N_t-D signal space, it was shown in [11] that for any symbol $\boldsymbol{s}$, there is only one symbol $\boldsymbol{p}$ at the largest squared Euclidean distance $4M$ to $\boldsymbol{s}$. Furthermore, there are M symbols $\{\boldsymbol{p}\}$ at the second largest squared Euclidean distance $4(M-1)$ to $\boldsymbol{s}$. Thus, for an ideal mapping ξ, over M possible symbols $\{\boldsymbol{p}\}$ whose labels differ in only 1 bit to that of $\boldsymbol{s}$, there is one symbol at squared Euclidean distance $4M$ and $(M-1)$ symbols at squared Euclidean distance $4(M-1)$ to $\boldsymbol{s}$. This implies the following lower bound on $\hat{\delta}(\mathbf{\Psi},\xi)$:

$$\begin{aligned}&\hat{\delta}(\mathbf{\Psi},\xi)\\ \geq\ &\frac{1}{M}\left(1\cdot\frac{1}{(4M)^{-N_r}}+(M-1)\cdot\frac{1}{(4(M-1))^{-N_r}}\right)\\ =\ &\frac{4^{-N_r}}{M}\left[M^{-N_r}+(M-1)^{-(N_r-1)}\right].\end{aligned} \tag{16}$$

It is simple to see that a mapping rule ξ that satisfies the following condition achieves the equality in (16), or equivalently, minimizes $\hat{\delta}(\mathbf{\Psi},\xi)$ over all possible mappings of the N_t-D hypercube $\mathbf{\Psi}$:

Condition 1: For any symbol $\boldsymbol{s}\in\mathbf{\Psi}$, let $\mathbf{\Psi}_{\boldsymbol{s}}$ be a set of M symbols $\{\boldsymbol{p}\}$ whose labels differ in only 1 bit to that of $\boldsymbol{s}$. In $\mathbf{\Psi}_{\boldsymbol{s}}$, there are one symbol at squared Euclidean distance $4M$ and $(M-1)$ symbols at squared Euclidean distances $4(M-1)$ to $\boldsymbol{s}$.

When combining with an 1-D mapping, a rate-1 code $\boldsymbol{G}$ is called *optimal* if it is invertible and the combination leads to a multi-D mapping ξ that satisfies *Condition 1*. In the following, this optimal code is determined for both anti-Gray and Gray mappings. For convenience, the notations $\boldsymbol{W}$ and $\boldsymbol{F}$ are used to indicate rate-1 code for anti-Gray and Gray mappings, respectively.

1) Optimal codes for anti-Gray mapping: When anti-Gray mapping is used, it can be easily verified that a group of 2 binary bits (b_{2i-1},b_{2i}), $1\leq i\leq N_t$, shall be mapped to a QPSK symbol $s_i=[2(b_{2i-1}\oplus b_{2i})-1,2b_{2i-1}-1,]$, where $\oplus$ denotes GF(2) addition. As a result, a symbol $\boldsymbol{s}\in\mathbf{\Psi}$ with label $\boldsymbol{v}$ carrying M bits $\boldsymbol{b}$, $\boldsymbol{b}=\boldsymbol{G}\cdot\boldsymbol{v}$, can be represented as:

$$\boldsymbol{s}=[2(b_1\oplus b_2)-1,2b_1-1,\ldots,2(b_{M-1}\oplus b_M)-1,2b_{M-1}-1]^\top. \tag{17}$$

One then has the following necessary condition for an optimal $\boldsymbol{W}$.

Condition 2: For any optimal $\boldsymbol{W}$, let $\boldsymbol{w}_k=[w_{1,k},\ldots,w_{M,k}]^\top$ be its kth column. Then

$$[w_{2i-1,k},w_{2i,k}]=[1,0] \tag{18}$$

for at least (N_t-1) values of i, $1\leq i\leq N_t$.

The proof that an optimal $\boldsymbol{W}$ satisfies *Condition 2* is quite simple. In particular, consider two symbols $\boldsymbol{s}=[s_1,\ldots,s_{N_t}]^\top$ and $\boldsymbol{p}=[p_1,\ldots,p_{N_t}]^\top$ whose labels $\boldsymbol{v}$ and $\boldsymbol{y}$ differ in only 1 bit at position k. For a given optimal $\boldsymbol{W}$, let $\boldsymbol{b}=\boldsymbol{W}\cdot\boldsymbol{v}$ and $\boldsymbol{a}=\boldsymbol{W}\cdot\boldsymbol{y}$. It then follows that:

$$\boldsymbol{b}\oplus\boldsymbol{a}=\boldsymbol{W}\cdot(\boldsymbol{v}\oplus\boldsymbol{y})=\boldsymbol{w}_k. \tag{19}$$

Since $\boldsymbol{W}$ is optimal, $||\boldsymbol{s}-\boldsymbol{p}||^2\geq 4(M-1)$. Equivalently, $||s_i-p_i||^2=8$ for at least (N_t-1) values of i, $1\leq i\leq N_t$. Furthermore, from (17), one has:

$$\begin{aligned}&||s_i-p_i||^2=\\ &4\left((b_{2i-1}-a_{2i-1})^2+((b_{2i-1}\oplus b_{2i})-(a_{2i-1}\oplus a_{2i}))^2\right).\end{aligned} \tag{20}$$

It can be observed from (20) that $||s_i-p_i||^2=8$ if and only if $[b_{2i-1}\oplus a_{2i-1},b_{2i}\oplus a_{2i}]=[1,0]$. In combining with (19), this result indicates that any optimal $\boldsymbol{W}$ satisfies *Condition 2*.

Condition 2 shows an important structure of an optimal $\boldsymbol{W}$. Based on it, the following proposition provides an optimal $\boldsymbol{W}$ for anti-Gray mapping.

Proposition 1: For anti-Gray mapping, the entries of the optimal rate-1 block code $\boldsymbol{W}$ are given as:

$$[w_{2i-1,k},w_{2i,k}]=\begin{cases}[1,0], & k=1,1\leq i\leq N_t\\ [1,0], & 1<k\leq M, i\neq(k+1)\ \text{div}\ 2, 1\leq i\leq N_t\\ [0,1], & 1<k\leq M, k\bmod 2=0, i=(k+1)\ \text{div}\ 2\\ [1,1], & 1<k\leq M, k\bmod 2=1, i=(k+1)\ \text{div}\ 2\end{cases} \tag{21}$$

Proof: First, let $\boldsymbol{z}=[z_1,\ldots,z_M]^\top$ be a vector of M binary bits and $z=z_1\oplus z_2\oplus\ldots\oplus z_M$. Consider the following linear combination:

$$\boldsymbol{x}=z_1\boldsymbol{w}_1\oplus z_2\boldsymbol{w}_2\oplus\ldots\oplus z_M\boldsymbol{w}_M \tag{22}$$

It then follows from (21) that:

$$\boldsymbol{x}=[z\oplus z_2,z_2,\ldots,z\oplus z_{2i},z_{2i-1}\oplus z_{2i},\ldots,z_M,z_{M-1}\oplus z_M]^\top \tag{23}$$

Therefore, $\boldsymbol{x}=\boldsymbol{0}$ if and only if $\boldsymbol{z}=\boldsymbol{0}$. As a result, all M columns of $\boldsymbol{W}$ are linearly independent, which make $\boldsymbol{W}$ invertible. Furthermore, let ξ be a mapping constructed from the combination of $\boldsymbol{W}$ and anti-Gray mapping. Consider two symbols $\boldsymbol{s}$ and $\boldsymbol{p}$ whose label differ in only 1 bit at position k. One has two separate cases as follows:

- If $k=1$, it can be verified that $||s_i-p_i||^2=8$ for all $1\leq i\leq N_t$, since $[w_{2i-1,k},w_{2i,k}]=[1,0]$. This makes $||\boldsymbol{s}-\boldsymbol{p}||^2=4M$

- If $k > 1$, $||s_i - p_i||^2 = 8$ for all $1 \le i \le N_t$ but $i = (k+1)$ div 2. When $i = (k+1)$ div 2, it follows from (21) and (20) that $||s_i - p_i||^2 = 4$. Therefore, $||\boldsymbol{s} - \boldsymbol{p}||^2 = 4(M-1)$.

Combining the above results, it can be concluded that the mapping ξ satisfies *Condition 1*. Since $\boldsymbol{W}$ is invertible and its combination with anti-Gray mapping results in a mapping that satisfies *Condition 1*, it is optimal. *Proposition 1* is thus proved. As an example, the optimal $\boldsymbol{W}$ for $N_t = 4$ can be expressed as:

$$\boldsymbol{W} = \begin{pmatrix} 1 & 0 & 1 & 1 & 1 & 1 & 1 & 1 \\ 0 & 1 & 0 & 0 & 0 & 0 & 0 & 0 \\ 1 & 1 & 1 & 0 & 1 & 1 & 1 & 1 \\ 0 & 0 & 1 & 1 & 0 & 0 & 0 & 0 \\ 1 & 1 & 1 & 1 & 1 & 0 & 1 & 1 \\ 0 & 0 & 0 & 0 & 1 & 1 & 0 & 0 \\ 1 & 1 & 1 & 1 & 1 & 1 & 1 & 0 \\ 0 & 0 & 0 & 0 & 0 & 0 & 1 & 1 \end{pmatrix}. \tag{24}$$

Besides the optimal $\boldsymbol{W}$ in (21), it is worth noting that by permuting any two columns of $\boldsymbol{W}$, another optimal code can also be obtained. The proof is omitted here for brevity of the presentation.

2) Optimal codes for Gray mapping: For a given optimal $\boldsymbol{W}$ in (21), define $\boldsymbol{F}$ as a $M \times M$ matrix over GF(2) whose elements are:

$$\begin{cases} f_{2i-1,k} = w_{2i-1,k} \oplus w_{2i,k} \\ f_{2i,k} = w_{2i-1,k} \end{cases} \tag{25}$$

The following proposition states the optimality of $\boldsymbol{F}$.

Proposition 2: The use of rate-1 code $\boldsymbol{F}$ in (25) together with Gray mapping results in the same mapping rule ξ attainted by combining rate-1 code $\boldsymbol{W}$ in (21) and anti-Gray mapping. Consequently, $\boldsymbol{F}$ in (25) is optimal for Gray mapping.

Proof: Let $\boldsymbol{v}$ be a vector of binary inputs. When $\boldsymbol{W}$ in (21) is used together with anti-Gray mapping, a symbol $\boldsymbol{s} \in \boldsymbol{\Psi}$ with label $\boldsymbol{v}$ carrying M bits $\boldsymbol{b}$, $\boldsymbol{b} = \boldsymbol{G} \cdot \boldsymbol{v}$, is given in (17). On the other hand, with rate-1 code $\boldsymbol{F}$ followed by Gray mapping, a symbol $\boldsymbol{p} \in \boldsymbol{\Psi}$ carrying M bits $\boldsymbol{a}$, $\boldsymbol{a} = \boldsymbol{F} \cdot \boldsymbol{v}$, can be expressed as:

$$\boldsymbol{p} = [2a_1 - 1, 2a_2 - 1, \ldots, 2a_{M-1} - 1, 2a_M - 1]^\top. \tag{26}$$

From (25), one has:

$$\begin{cases} a_{2i-1} = \boldsymbol{f}^{(2i-1)} \cdot \boldsymbol{v} = \left(\boldsymbol{w}^{(2i-1)} \oplus \boldsymbol{w}^{(2i)}\right) \cdot \boldsymbol{v} = b_{2i-1} \oplus b_{2i} \\ a_{2i} = \boldsymbol{f}^{(2i-1)} \cdot \boldsymbol{v} = \boldsymbol{w}^{(2i-1)} \cdot \boldsymbol{v} = b_{2i-1} \end{cases} \tag{27}$$

where $\boldsymbol{f}^{(k)}$ and $\boldsymbol{w}^{(k)}$ are the kth rows of $\boldsymbol{F}$ and $\boldsymbol{W}$, respectively. It then follows from (17), (26), and (27) that $\boldsymbol{s} = \boldsymbol{p}$. It means that a combination of either $\boldsymbol{F}$ and Gray mapping or $\boldsymbol{W}$ and anti-Gray mapping leads to the same mapping rule ξ. *Proposition 2* is proved.

Combining the above results, it can be concluded that the combination of rate-1 code $\boldsymbol{W}$ in (21) followed by anti-Gray mapping is equivalent to the combination of rate-1 code $\boldsymbol{F}$ in (25) and Gray mapping. Furthermore, these combinations minimize $\hat{\delta}(\boldsymbol{\Psi}, \xi)$ in (15) over all possible mappings of $\boldsymbol{\Psi}$. It means that for a given outer mixed code, the proposed concatenation is optimal as far as the asymptotic performance is concerned.

TABLE I
ASYMPTOTIC GAINS WITH RESPECT TO GRAY MAPPING

$N_t \times N_r$	Proposed scheme	Best mapping obtained in [13]
4×4	8.51dB	7.26dB
3×4	7.10dB	6.16dB
3×2	7.11dB	6.24dB
3×1	7.11dB	6.52dB

To further justify the advantage of the above mapping construction over other mapping rules, the so-called asymptotic gain between two mappings defined in [13] can be used. In particular, the asymptotic gain of mapping ξ_1 with respect to mapping ξ_2 is calculated as [13]:

$$\text{Gain}_{\text{dB}} = \frac{1}{N_r} 10 \log_{10} \left(\frac{\hat{\delta}(\boldsymbol{\Psi}, \xi_2)}{\hat{\delta}(\boldsymbol{\Psi}, \xi_1)} \right). \tag{28}$$

It is not hard to verify that the asymptotic gain of the developed mapping with respect to Gray mapping is:

$$\text{Gain}_{\text{dB}}^{\text{opt}} = \frac{1}{N_r} 10 \log_{10} \left(\frac{M}{M^{-N_r} + (M-1)^{-(N_r-1)}} \right). \tag{29}$$

Table I compares $\text{Gain}_{\text{dB}}^{\text{opt}}$ with the asymptotic gain with respect to Gray mapping of the best mapping rules found by search techniques in [13]. It is not surprising to observe from Table I that the proposed scheme provides a better asymptotic gain. It is because our construction leads to a globally optimal mapping, whilst computer-based searching methods usually end up with only a local optimum, especially in a high dimensional signal space.

IV. OUTER MIXED CODE DESIGN USING EXIT CHARTS

The analysis presented in Section III is only useful to predict the error performance of an iterative demodulation and decoding scheme at the BER floor region. In this region, a reasonably low BER can be achieved at a sufficiently high SNR value. This however might not be of practical interest. In order to examine whether an iterative demodulation and decoding system can achieve near-capacity, one needs to take into account the convergence behavior in the turbo pinch-off, or water-fall, region, where a significant BER decrease is observed over iterations (please see [28] and references therein for detailed discussions).

This section analyzes the convergence property of the proposed scheme at the turbo pinch-off region by means of extrinsic information transfer (EXIT) chart [14]. Following the same notations as in [14], let I_{A_1} and I_{E_1} denote the mutual information between the *a priori* LLR and the transmitted coded bit, and between extrinsic LLR and the transmitted coded bit at the input and output of the detector, respectively. Similarly, let I_{E_2} and I_{A_2} be the mutual information representing the *a priori* knowledge and the extrinsic information of the coded bits at the input and output of the SISO decoder. After being deinterleaved, the extrinsic output of the detector is used as the *a priori* input to the decoder, i.e., $I_{A_2} = I_{E_1}$. Furthermore, after being interleavered, the extrinsic information of the decoder becomes the *a priori* information to be provided to the detector, i.e., $I_{A_1} = I_{E_2}$.

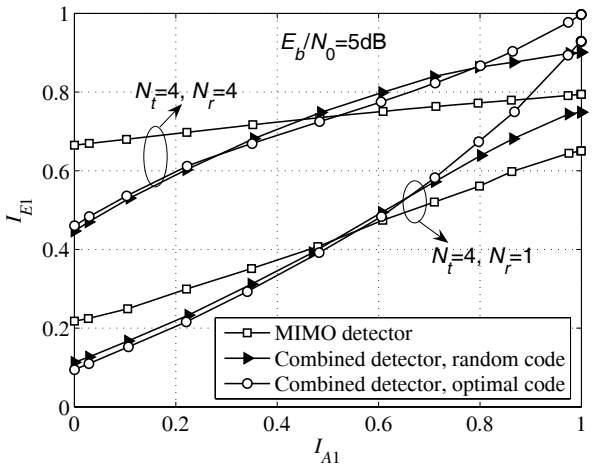

Fig. 2. The MIMO and combined detector EXIT curves at E_b/N_0=5dB.

In the following, the difference between the conventional MIMO detector with Gray mapping employed in coded modulation systems using powerful turbo-like codes [3]–[6] and the combined detector considered in this paper is first demonstrated with the aid of EXIT curves. Note that the MIMO detector can also be understood as a combined detector in which the rate-1 code is an identity matrix. Furthermore, the combined detector of optimal codes is the same for both cases of rate-1 code $\boldsymbol{W}$ in (21) with anti-Gray mapping and rate-1 code $\boldsymbol{F}$ in (25) with Gray mapping, since they are equivalent. Then a combination of the combined detector of optimal codes and a mixture of simple convolutional or repetition decoders, with which close-capacity performance can be achieved, is proposed by having the combined detector EXIT curve matched to the decoder EXIT curve. We only use the same rate-1/2 component codes, which results in an overall rate $r_c = 1/2$ outer mixed code. The analysis and design can be easily extended to other code rates. The ratio of energy per information bit at the receiver over noise power, E_b/N_0, is defined as [3], [4]:

$$E_b/N_{0(\text{dB})} = E_s/N_{0(\text{dB})} + 10\log 10\frac{N_r}{r_c N_t m_c}, \tag{30}$$

where E_s is total energy used over N_t transmit antennas and $m_c = 2$ for QPSK.

A. EXIT curves of the MIMO detector and combined detector

Fig. 2 shows EXIT curves of the MIMO detector and combined detectors for two different rate-1 invertible codes at $E_b/N_0 = 5$dB with $N_t = 4$ and different numbers of receive antennas to demonstrate the effectiveness of the optimal codes developed earlier. Besides the optimal ones, we also consider the below invertible code that is generated randomly:

$$\widetilde{\boldsymbol{W}} = \begin{pmatrix} 0 & 1 & 0 & 0 & 0 & 1 & 0 & 1 \\ 1 & 1 & 0 & 0 & 1 & 1 & 1 & 0 \\ 1 & 0 & 0 & 1 & 0 & 0 & 0 & 0 \\ 1 & 0 & 1 & 1 & 0 & 0 & 0 & 0 \\ 1 & 0 & 0 & 0 & 0 & 1 & 1 & 0 \\ 1 & 0 & 0 & 0 & 1 & 1 & 1 & 0 \\ 0 & 0 & 1 & 0 & 0 & 0 & 0 & 1 \\ 0 & 0 & 1 & 0 & 0 & 0 & 0 & 1 \end{pmatrix}. \tag{31}$$

For a 4×4 channel, it can be seen from Fig. 2 that the EXIT curve of the MIMO detector is flat compared to those of the two combined detectors. Therefore, the use of Gray mapping alone is matched to powerful turbo-like codes, including LDPC codes optimized for binary input channels. This is because EXIT curves of these powerful codes are also almost horizontal [4], [6]. However, for an asymmetric channel, i.e., when $N_t > N_r$, the EXIT curve of the MIMO detector exhibits a steeper slope. This phenomenon causes a performance degradation when Gray mapping is used together with the above-mentioned turbo-like codes [4], [9]. This problem can be overcome by using well-designed irregular LDPC or RA codes as recently proposed in [4], [5].

In the case of the combined detectors, it can be observed from Fig. 2 that the EXIT curves of both combined detectors exhibit higher slopes over that of the MIMO detector. As shown in Appendix A, the use of an optimal code maximizes the bitwise mutual information with perfect *a priori* information, i.e., $I_{E_1}(I_{A_1} = 1)$. Therefore, $I_{E_1}(I_{A_1} = 1)$ attained by using the optimal codes is much larger than that of both the MIMO detector and the combined detector using the code $\widetilde{\boldsymbol{W}}$. Since the block codes are of rate 1, the areas under the EXIT curves of the combined detectors and MIMO detector must be equal [29]. Consequently, the combined detector's EXIT curve of the optimal codes has the highest slope, with the largest mutual information at the right end of the curve. This makes the combination of either rate-1 code $\boldsymbol{W}$ in (21) with anti-Gray mapping or rate-1 code $\boldsymbol{F}$ in (25) with Gray mapping a perfect match to a simple outer code, which also have decayed EXIT curves. Certainly, a different outer code can also be constructed to work well with the code $\widetilde{\boldsymbol{W}}$. However, due to a flatter slope of the combined detector's EXIT curve, a more complicated outer code is required. As shown in the next subsection, the optimal codes can be indeed combined with very simple outer mixed codes of short-memory length convolutional codes or repetition codes to achieve near-capacity performance over both symmetric and asymmetric multiple-antenna channels.

B. EXIT curve matching

This subsection applies the EXIT chart technique [14] to select a suitable mixed code for the combined detector of the optimal rate-1 codes. This detector is referred to as the optimal combined detector hereafter. By using EXIT charts, both EXIT curves of the optimal combined detector and decoder are placed in the same graph, but the axes of the EXIT curve of the decoder are swapped [14] so that the convergence behavior of the concatenation scheme can be well visualized. It should be

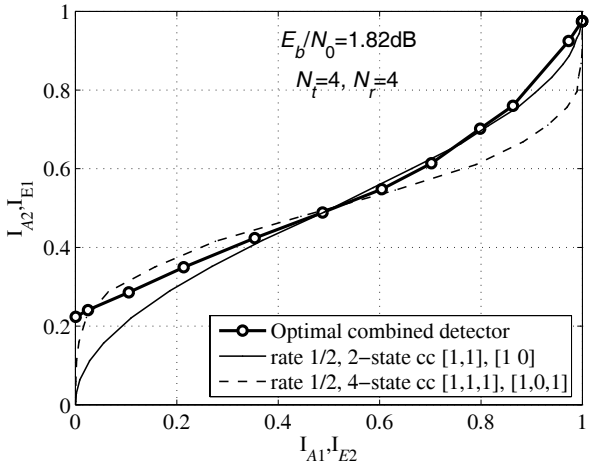

Fig. 3. EXIT charts of the optimal combined detector with $N_t = N_r = 4$ at E_b/N_0=1.82dB, rate-1/2, 2-state cc with $\mathbf{g}_1 = [1, 1]$ and $\mathbf{g}_2 = [1, 0]$, and rate-1/2 4-state cc with $\mathbf{g}_1 = [1, 1, 1]$ and $\mathbf{g}_2 = [1, 0, 1]$.

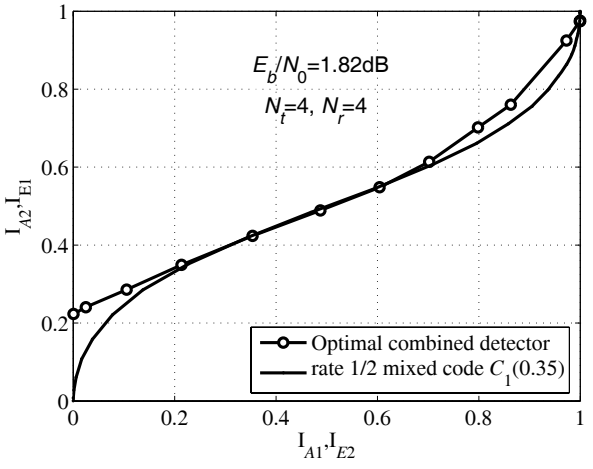

Fig. 4. EXIT charts of the optimal combined detector with $N_t = N_r = 4$ at E_b/N_0=1.82dB and a rate-1/2 mixed code $C_1(0.35)$, which is a mixture of rate-1/2 4-state and 2-state codes with code doping ratio $\alpha = 0.35$.

mentioned that for the system under consideration, the EXIT curve of a rate-r_c mixed code does not depend on SNR and always crosses the middle point $(0.5, r_c)$ [14].

We first examine the symmetric case with $N_t = N_r = 4$. Fig. 3 plots the EXIT curve of the optimal combined detector at E_b/N_0=1.82dB and the EXIT curves of two standard rate-1/2, 2-state convolutional code with generator polynomials $\mathbf{g}_1 = [1, 1]$ and $\mathbf{g}_2 = [1, 0]$, and rate-1/2, 4-state convolutional code with generator polynomials $\mathbf{g}_1 = [1, 1, 1]$ and $\mathbf{g}_2 = [1, 0, 1]$. The above SNR is chosen to make sure that the middle point of the detector EXIT curve $I_{E_1}(0.5)$ is larger than 0.5. It is clear from Fig. 3 that the EXIT curve of the standard rate-1/2, 4-state convolutional code with generator polynomials $\mathbf{g}_1 = [1, 1, 1]$ and $\mathbf{g}_2 = [1, 0, 1]$ does not fit well to the detector EXIT curve, since the two EXIT curves quickly intersect and the intersection point falls in the lower left quadrant of the EXIT plane. Because the EXIT curve of a more powerful rate-1/2 convolutional code exhibits a sharper slope at the beginning, it is straightforward to see that stronger convolutional codes are not suitable either. The EXIT curve of rate-1/2, 2-state convolutional code intersects the optimal combined detector EXIT curve in the upper right quadrant of the EXIT plane, but at a low mutual information, which does not guarantee low BER.

To overcome the above disadvantages, a mixed code of the two standard convolutional codes, denoted as $C_1(\alpha)$, can be used to achieve better curve matching. In particular, Fig. 4 shows the EXIT curve of the optimal combined detector at E_b/N_0=1.82dB and the EXIT curve of $C_1(0.35)$, which is a mixture of 4-state and 2-state codes with code doping ratio $\alpha = 0.35$. It is interesting to see that the EXIT curve of this mixed code matches very well to the detector EXIT curve. The two EXIT curves do not intersect until reaching the ending point $I_{A_1}(1)$ with very high mutual information, leading to a low BER. This match is very similar to that obtained in [4], [5] using an irregular LDPC or RA code and Gray mapping alone,

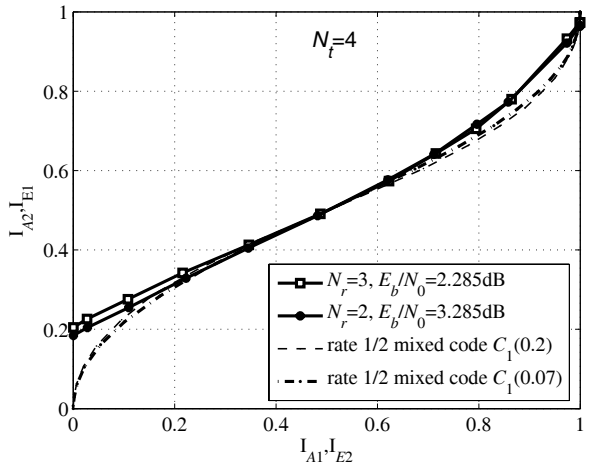

Fig. 5. EXIT charts of the optimal combined detector in various asymmetric scenarios using $N_t = 4$ and $N_r = 3$ at E_b/N_0=2.285dB, $N_t = 4$ and $N_r = 2$ at E_b/N_0=3.285dB, and rate-1/2, mixed codes $C_1(0.2)$ and $C_1(0.07)$.

where the curves fit at the pinch-off limit[3] $E_b/N_0 = 1.8$dB. Furthermore, this curve fit happens close to the capacity limit, which is at $E_b/N_0 = 1.47$dB.

In the case of asymmetric configurations, mixed codes can also be effectively applied to match with the optimal combined detector EXIT curves. Fig. 5 provides the optimal combined detector EXIT curves in two asymmetric setups i) $N_t = 4$ and $N_r = 3$; and ii) $N_t = 4$ and $N_r = 2$ at E_b/N_0=2.285dB and E_b/N_0=3.285dB, respectively, and the EXIT curves of mixed codes $C_1(0.2)$ and $C_1(0.07)$ of 4-state and 2-state codes. Observe that the EXIT curves are matched very well in all cases. Similar to the symmetric scenario, these results are very comparable to those achieved in [4], [5].

C. Further Results with Asymmetric Setups

It is of further interest to consider an asymmetric antenna setup in which multiple antennas are only equipped at the

[3]The pinch-off point is understood at the smallest E_b/N_0 at which two EXIT curves fit.

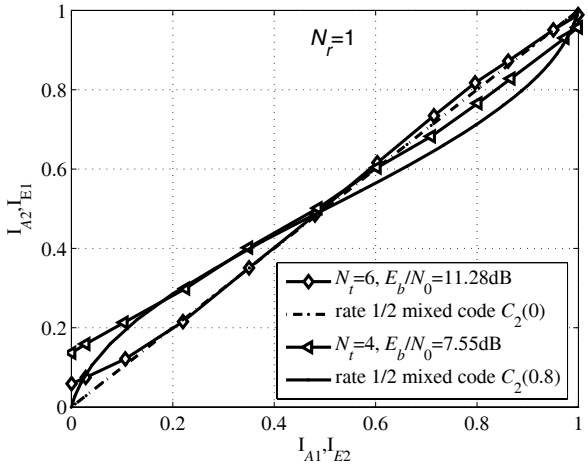

Fig. 6. EXIT curves of the optimal combined detector with (N_t=6, N_r=1) and (N_t=4, N_r=1) antennas at E_b/N_0=11.28dB and E_b/N_0=7.55dB, respectively, and EXIT curves of rate-1/2 mixed codes $C_2(0)$ and $C_2(0.8)$.

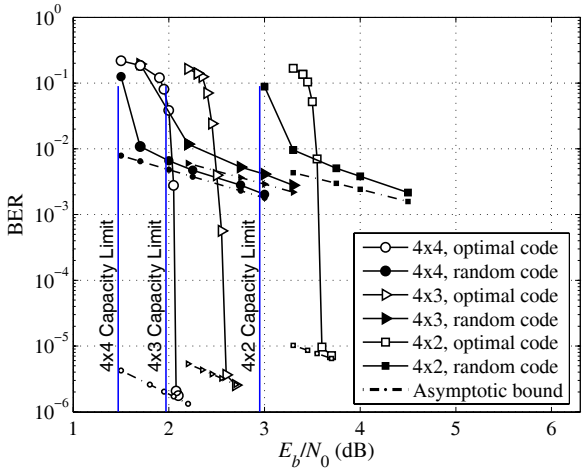

Fig. 7. BER performance of the proposed systems equipped with $N_t = 4$ transmit and $N_r = 4$, $N_r = 3$, and $N_r = 2$ receive antennas. The outer codes are rate-1/2 mixed codes $C_1(0.35)$, $C_1(0.2)$, and $C_1(0.07)$, respectively.

base-station. This antenna configuration is very common in the downlink of a cellular system, where it is physically not possible to place multiple antennas on a small handset. Under this scenario, it can be seen from Fig. 2 that the combined detector EXIT curves of the optimal rate-1 codes experience much higher slope, especially when the number of transmit antennas is large. This suggests that a simpler mixed code should be used for a good convergence.

The EXIT curves of the optimal combined detector for two antenna configurations i) N_t=6, N_r=1[4]; and ii) N_t=4, N_r=1 antennas at E_b/N_0=11.28dB and E_b/N_0=7.55dB, respectively, are shown in Fig. 6. Note that the corresponding capacity limits are at E_b/N_0=10.77dB and E_b/N_0=6.65dB. Also plotted in Fig. 6 are the EXIT curves of rate-1/2 mixed codes $C_2(0.8)$ and $C_2(0)$ of a component rate-1/2, 2-state convolutional code and rate-1/2 repetition code with code doping ratios $\alpha = 0.8$ and $\alpha = 0$, respectively. Note that the code $C_2(0)$ corresponds to the case of a single rate-1/2 repetition code. It can be seen from Fig. 6 that $C_2(0.8)$ is a good match for the system with N_t=4 and N_r=1. Furthermore, it is observed from Fig. 6 that the optimal combined detector EXIT curve of the (N_t=6, N_r=1) setup fits well to that of $C_2(0)$, which is the simplest possible code. More impressively, this curve match is achieved at only 0.5dB away from the capacity limit.

Table II summarizes the results obtained in this section and those in [4], [5] for comparison. The respective capacity limits are also provided. Clearly, the pinch-off E_b/N_0 in Table II shows that the concatenation scheme employing only simple outer mixed codes and inner rate-1 block code can approach close to the capacity limit for the both symmetric and asymmetric antenna setups. The convergence and asymptotic properties discussed in this section are verified by the BER performances in the next section.

Before closing this section, it should be pointed out that the derived optimal codes in (21) and in (25) are to optimize the error-floor performance for a given outer code, or equivalently, to maximize $I_{E_1}(I_{A_1} = 1)$ for the combined detector. There might be other rate-1 codes that achieve a comparable $I_{E_1}(I_{A_1} = 1)$ while providing a different combined detector's EXIT curve. These codes, if exist, can be matched with a different set of component codes in the turbo pinch-off region for achieving closer to the capacity limit. To solve this challenging problem, care should be taken in optimizing the code over all values of prior information I_{A_1}. This interesting topic therefore deserves a further investigation.

[4]Such a 6×1 system requires a complicated APP detector at the receiver. This single receive antenna system typically requires a low-cost receiver. As such, a simpler decoder, such as the list sphere decoder in [3], could be used as an alternative to the APP detector.

V. Illustrative Results

This section provides numerical and simulation results to verify the analysis made in the previous sections and to demonstrate the excellent performance achieved by the proposed systems using the optimal rate-1 code. A random interleaver of length 1×10^5, which is the same to those considered in [4], [5], is used. Each point in the BER curves is simulated with 6×10^6 to 10^9 coded bits. In the computation of the asymptotic bound for P_b in (5) and (6), if a convolutional code is used as a component code, its first 20 Hamming distances in the distance spectrum are included.

Fig. 7 shows the BER performances with 80 iterations of the concatenation scheme using $N_t = 4$ transmit antennas and $N_r = 4$, $N_r = 3$, and $N_r = 2$ receive antennas. Besides the optimal rate-1 code, the BER performances for the system using the randomly generated code $\widetilde{\boldsymbol{W}}$ in (31) are also provided for comparison. The outer codes are rate-1/2 mixed codes $C_1(0.35)$, $C_1(0.2)$, and $C_1(0.07)$, respectively. For the system employing the optimal rate-1 code, it can be seen from Fig. 7 that the analytical results obtained by EXIT charts agree with the BER curves. In particular, the turbo pinch-off region happens around E_b/N_0=2dB, E_b/N_0=2.48dB, and E_b/N_0=3.50dB and near-capacity performances can be achieved, given the practical BER level of 10^{-4} or 10^{-5} as a target. On the other hand, the system using the code $\widetilde{\boldsymbol{W}}$ experiences a very high error floor and it operates far from the

TABLE II
CAPACITY AND PINCH-OFF POINTS OF THE PROPOSED SYSTEM AND THOSE ACHIEVED IN [4], [5].

$N_t \times N_r$ channel	Proposed system Outer mixed code	Proposed system Curves fit at E_b/N_0	Schemes in [4], [5] Curves fit at E_b/N_0	Capacity E_b/N_0
4×4	$C_1(0.35)$	1.82dB	1.80dB	1.47dB
4×3	$C_1(0.20)$	2.285dB	2.30dB	1.97dB
4×2	$C_1(0.07)$	3.285dB	3.30dB	2.95dB
4×1	$C_2(0.8)$	7.55dB	7dB	6.65dB
6×1	$C_2(0)$	11.28dB	N/A	10.77dB

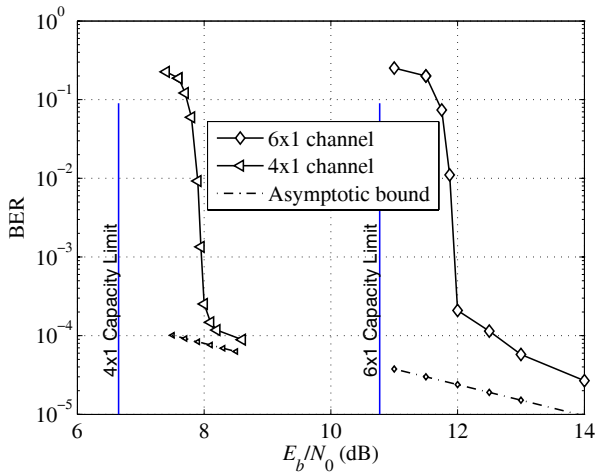

Fig. 8. BER performances with 50 iterations of the proposed systems equipped with $N_t = 6$ and $N_t = 4$ transmit antennas, and $N_r = 1$ receive antenna. The outer codes are rate-1/2 mixed codes $C_2(0)$ and $C_2(0.8)$, respectively.

capacity limit. Further performance improvement for such a system can only be achieved by using more complicated outer codes as discussed earlier. The tightness of the asymptotic bound in the error floor region is clearly observed for all the systems under consideration. This makes the bound effective in predicting the error performance at reasonable high SNR regions.

Similar near-capacity performances are also obtained in the asymmetric antenna configurations when there is only a single receive antenna at the receiver. In particular, Fig. 8 plots the BER performance with 50 iterations of the 6×1 and 4×1 systems using the optimal rate-1 code. The corresponding outer codes for the two systems are the rate-1/2 mixed codes $C_2(0)$ and $C_2(0.8)$, respectively. The results appear impressive for such simple systems, since the turbo pinch-off happens very close to the capacity limit. The error floor kicks in at the BER of 10^{-4}, which is still reasonable. Note that the derived asymptotic bound slightly overestimates the actual BER performance for the two systems. It is merely due to the reason that in the range of the SNR shown in Fig. 8, a perfect *a priori* information of coded bits has not been achieved, which can also be seen by EXIT charts in Fig. 6. The tightness of the error bound is indeed observed at a higher SNR region, which still makes the error bound useful in estimating the BER in the error-floor region.

Table III briefly summarizes the simulation results for the proposed scheme using the optimal rate-1 code where the BER of 10^{-4} is measured. The results obtained in [4], [5] using irregular LDPC and RA codes, as well as those attained by using the standard UMTS parallel concatenated turbo code constructed from memory-three constituent codes, with feedback and feedforward generator polynomials $[1, 0, 1, 1]$ and $[1, 1, 0, 1]$ are also included. It can be seen that the simple concatenation scheme achieves very comparable error performances to those in [4], [5]. Furthermore, it outperforms the standard UMTS turbo coded system, especially in the asymmetric scenarios.

VI. CONCLUSIONS

This paper introduced a novel coded modulation scheme over multiple-antenna channels with QPSK using a concatenation of a simple outer mixed code and a short rate-1 linear block code followed by either 1-D anti-Gray or Gray mapping. In the error-floor region, the error bound and design criterion were first derived, which can be used to accurately predict the error performance. Optimal rate-1 block codes were then developed for both anti-Gray and Gray mappings to achieve the best asymptotic performance. Furthermore, it has been shown through EXIT chart analysis that the proposed system achieves comparable performances to those using well-designed LDPC and RA codes in the turbo pinch-off region. As a result, it approaches near-capacity performance over both symmetric and asymmetric multiple-antenna channels, and thereby, outperforms a scheme employing a standard parallel concatenated (turbo) code at a lower decoding complexity. The performance improvement was shown to be more significant when there are more transmit antennas than receive antennas. The proposed system is therefore an attractive alternative for other coded modulation schemes over multiple-antenna wireless fading channels.

Finally, it is worthwhile mentioning that it is interesting to extend the proposed technique to higher modulation schemes, such as 8-PSK or 16-QAM. The problem is currently under investigation for 8-PSK, using the fact that this modulation scheme can be decomposed into two sets of QPSK constellations.

ACKNOWLEDGEMENT

The authors would like to thank the anonymous reviewers for helpful comments and suggestions that improve the presentation of the paper.

TABLE III
ERROR PERFORMANCE COMPARISON FOR THE PROPOSED SYSTEM AND THOSE IN [4], [5].

$N_t \times N_r$ channel	Proposed system BER 10^{-4} at E_b/N_0	Schemes in [4], [5] BER 10^{-4} at E_b/N_0	UMTS turbo-coded system BER 10^{-4} at E_b/N_0
4×4	2.05dB	1.95dB	2.40dB
4×3	2.52dB	2.45dB	3.20dB
4×2	3.56dB	3.60dB	5.40dB
4×1	8.10dB	7.90dB	13.80dB

APPENDIX A
BITWISE MUTUAL INFORMATION WITH PERFECT A PRIORI INFORMATION OF THE COMBINED DETECTOR

For a given constellation $\boldsymbol{\Psi}$ and mapping rule ξ, it was shown in [14] that the bitwise mutual information with perfect priori information is equal to $I_{E_1}(I_{A_1}=1)$. By interpreting the combination of rate-1 code and 1-D mapping as a multi-D mapping ξ, $I_{E_1}(I_{A_1}=1)$ can be calculated as follows:

$$I_{E_1}(I_{A_1}=1)=\frac{1}{M2^M}\sum_{\boldsymbol{s}\in\boldsymbol{\Psi}}\sum_{k=1}^{M} I_k(\boldsymbol{s},\boldsymbol{p}), \tag{32}$$

where $I_k(\boldsymbol{s},\boldsymbol{p})$ is the average mutual information of a BPSK-like constellation consisting of two signal points $\boldsymbol{s}$ and $\boldsymbol{p}$ whose labels differ in only 1 bit at position k. Due to the symmetry of a BPSK-like constellation, the conditional $I_k(\boldsymbol{s},\boldsymbol{p})|\boldsymbol{H}$ for a given channelization $\boldsymbol{H}$ can be expressed as:

$$\begin{aligned} &I_k(\boldsymbol{s},\boldsymbol{p})|\boldsymbol{H} \\ &= 1-\left[\frac{1}{(\pi N_0)^{N_r}}\int_{\boldsymbol{r}\in\mathcal{C}^{N_r}}\exp\left(-\frac{||\boldsymbol{r}-\boldsymbol{H}\cdot\boldsymbol{s}||^2}{N_0}\right)\right. \\ &\left.\times\log\left(1+\exp\left(\frac{||\boldsymbol{r}-\boldsymbol{H}\cdot\boldsymbol{s}||^2-||\boldsymbol{r}-\boldsymbol{H}\cdot\boldsymbol{p}||^2}{N_0}\right)\right)\mathrm{d}\boldsymbol{r}\right]. \end{aligned} \tag{33}$$

By using the symmetric cut-off rate and Jensen inequality as similar to the analysis in [30], $I_k(\boldsymbol{s},\boldsymbol{p})$ can be approximated as:

$$\begin{aligned} &I_k(\boldsymbol{s},\boldsymbol{p}) \\ \sim\ & 1-\log\left(1+E_{\boldsymbol{H}}\left[\exp\left(-\frac{||\boldsymbol{H}\cdot(\boldsymbol{s}-\boldsymbol{p})||^2}{4N_0}\right)\right]\right) \\ =\ & 1-\log\left(1+\left(1+\frac{||\boldsymbol{s}-\boldsymbol{p}||^2}{4N_0}\right)^{-N_r}\right). \end{aligned} \tag{34}$$

By substituting $I_k(\boldsymbol{s},\boldsymbol{p})$ from (34) to (32), it is observed that the expression in (32) is similar to the design criteria in (13) and (15). Since the combination of either rate-1 block code $\boldsymbol{W}$ in (21) with anti-Gray mapping or rate-1 block code $\boldsymbol{F}$ in (25) with Gray mapping minimizes $\hat{\delta}(\boldsymbol{\Psi},\xi)$ in (15), it is clear that $I_{E_1}(I_{A_1}=1)$ of the combined detector can also be maximized, and therefore, substantially outperforms that of the MIMO detector.

REFERENCES

[1] G. J. Foschini, "Layered space-time architecture for wireless communication in a fading environment when using multi-element antennas," *Bell Labs. Tech. J.*, vol. 1, pp. 41-59, Feb. 1996.

[2] I. E. Telatar, "Capacity of multi-antenna Gaussian channels," *European Trans. Telecommun. Related Technol.*, vol. 10, pp. 585-595, Nov. 1999.

[3] B. M. Hochwald and S. ten Brink, "Achieving near-capacity on mutiple-antenna channel," *IEEE Trans. Commun.*, vol. 51, pp. 389-399, Mar. 2003.

[4] S. ten Brink, G. Kramer, and A. Ashikhmin, "Design of low-density parity-check codes for modulation and detection," *IEEE Trans. Commun.*, vol. 52, pp. 670-678, Apr. 2004.

[5] S. ten Brink and G. Kramer, "Design of repeat accumulate codes for iterative detection and decoding," *IEEE Trans. Signal Process.*, vol. 51, pp. 2764–2772, Nov. 2003.

[6] J. Hou, P. H. Siegel, and L. B. Milstein, "Design of multi-input multi-output systems based on low-density parity-check codes," *IEEE Trans. Commun.*, vol. 53, pp. 601-611, Apr. 2005.

[7] E. Zehavi, "8-PSK trellis codes for a Rayleigh fading channel," *IEEE Trans. Commun.*, vol. 40, pp. 873-883, May 1992.

[8] G. Caire, G. Taricco, and E. Biglieri, "Bit-interleaved coded modulation," *IEEE Trans. Inf. Theory*, vol. 44, pp. 927-946, May 1998.

[9] S. ten Brink and B. M. Hochwald, "Detection thresholds of iterative MIMO processing," in *Proc. IEEE Int. Symp. Inf. Theory*, Lausanne, Switzerland, July 2002, p. 22.

[10] N. H. Tran and H. H. Nguyen, "Improving the performance of BICM-ID systems by mapping on the hypercube," in *Proc. IEEE Veh. Technol. Conf.*, Los Angeles, USA, Sept. 2004, pp. 1299-1303.

[11] ——, "Design and performance of BICM-ID systems with hypercube constellations," *IEEE Trans. Wireless Commun.*, vol. 5, pp. 1169-1179, May 2006.

[12] F. Simoens, H. Wymeersch, H. Bruneel, and M. Moeneclaey, "Multi-dimensional mapping for bit-interleaved coded modulation with BPSK/QPSK signaling," *IEEE Commun. Lett.*, vol. 9, May 2005.

[13] N. Gresset, J. Boutros, and L. Brunel, "Multidimensional mappings for iteratively decoded BICM on multiple-antenna channels," *IEEE Trans. Inf. Theory*, vol. 51, pp. 3337-3346, Sept. 2005.

[14] S. ten Brink, "Designing iterative decoding schemes with the extrinsic information chart," *AEU Int. J. Electron. Commun.*, vol. 54, pp. 389-398, Sept. 2000.

[15] ——, "Design of repeat-accumulate codes for iterative detection and decoding," *Electron. Lett.*, vol. 36, pp. 1293-1294, July 2000.

[16] V. Tarokh, N. Seshadri, and A. R. Calderbank, "Space-time codes for high data rate wireless communication: performance criterion and code construction," *IEEE Trans. Inf. Theory*, vol. 44, pp. 744-765, Mar. 1998.

[17] V. Tarokh, H. Jafarkhani, and A. R. Calderbank, "Space-time block codes from orthogonal designs," *IEEE Trans. Inf. Theory*, vol. 45, pp. 1456-1467, July 1999.

[18] B. Hassibi and B. Hochwald, "High-rate codes that are linear in space and time," *IEEE Trans. Inf. Theory*, vol. 48, pp. 1804-1824, July 2002.

[19] H. E. Gamal and M. O. Damen, "Universal space-time coding," *IEEE Trans. Inf. Theory*, vol. 49, pp. 1097-1119, May 2003.

[20] S. ten Brink, "Code doping for triggering iterative decoding convergence," in *Proc. IEEE Int. Symp. Inf. Theory*, Washington, DC, USA, June 2001, p. 235.

[21] M. Tuchler and J. Hagenauer, "EXIT charts of irregular codes," in *Proc. Conf. Inf. Sciences Syst.*, Princeton University, USA, Mar. 2002, pp. 1-6.

[22] F. Brännström and Lars K. Rasmussen, "Classification of unique mappings for 8PSK based on bit-wise distance spectra," *IEEE Trans. Inf. Theory*, vol. 53, pp. 1131-1145, Mar. 2009.

[23] A. Dejonghe and L. Vanderdorpe, "Turbo-equalization for multilevel modulation: an efficient low-complexity scheme," in *Proc. IEEE Int. Conf. Commun.*, New York, USA, Apr. 2002, pp. 1863-1867.

[24] A. Matache, C. Jones, and R. D. Wesel, "Reduced complexity MIMO detectors for LDPC coded systems," in *Proc. IEEE Military Commun. Conf.*, Monterey, CA, USA, Oct. 2004, pp. 1073-1079.

[25] L. R. Bahl, J. Cocke, F. Jelinek, and J. Raviv, "Optimal decoding of linear codes for minimizing symbol error rate," *IEEE Trans. Inf. Theory*, vol. IT-20, pp. 284-287, Mar. 1974.

[26] S. Benedetto, D. Divsalar, G. Montorsi, and F. Pollara, "A soft-input soft-output APP module for iterative decoding of concatenated codes," *IEEE Commun. Lett.*, vol. 1, pp. 22-24, Jan. 1997.
[27] X. Li, A. Chindapol, and J. A. Ritcey, "Bit-interleaved coded modulation with iterative decoding and 8PSK signaling," *IEEE Trans. Commun.*, vol. 50, pp. 1250-1257, Aug. 2002.
[28] S. ten Brink, "Convergence behavior of iteratively decoded parallel concatenated codes," *IEEE Trans. Commun.*, vol. 49, pp. 1727-1737, Oct. 2001.
[29] J. Hagenauer, "The EXIT chart—introduction to extrinsic information transfer in iterative processing," in *Proc. 12th European Signal Process. Conf. (EUSIPCO)*, 2004, pp. 1541-1548.
[30] E. Baccarelli and A. Fasano, "Some simple bounds on the symmetric capacity and outage probability for QAM wireless channels with Rice and Nakagami fadings," *IEEE J. Sel. Areas Commun.*, vol. 18, pp. 361-368, Mar. 2000.

Nghi H. Tran received the B.Eng. degree from Hanoi University of Technology, Vietnam in 2002, the M.Sc. degree (with Graduate Thesis Award) and the Ph.D. degree from the University of Saskatchewan, Canada in 2004 and 2008, respectively, all in electrical engineering. Since May 2008, he has been working at McGill University, Canada as a Postdoctoral Scholar under a prestigious Natural Sciences and Engineering Research Council of Canada (NSERC) Postdoctoral Fellowship. Dr. Tran's research interests span the areas of digital communications, and communication and network information theory.

Tho Le-Ngoc (Fellow IEEE) obtained his B.Eng. (with Distinction) in Electrical Engineering in 1976, his M.Eng. in Microprocessor Applications in 1978 from McGill University, Montreal, and his Ph.D. in Digital Communications 1983 from the University of Ottawa, Canada. During 1977-1982, he was with Spar Aerospace Limited as a Design Engineer and then a Senior Design Engineer, involved in the development and design of the microprocessor-based controller of Canadarm (of the Space Shuttle), and SCPC/FM, SCPC/PSK, TDMA satellite communications systems. During 1982-1985, he was an Engineering Manager of the Radio Group in the Department of Development Engineering of SRTelecom Inc., developed the new point-to-multipoint DA-TDMA/TDM Subscriber Radio System SR500. He was the System Architect of this first digital point-to-multipoint wireless TDMA system. During 1985-2000, he was a Professor in the Department of Electrical and Computer Engineering of Concordia University. Since 2000, he has been a Professor in the Department of Electrical and Computer Engineering of McGill University. His research interest is in the area of broadband digital communications. He is the recipient of the 2004 Canadian Award in Telecommunications Research, and recipient of the IEEE Canada Fessenden Award 2005. He holds a Canada Research Chair (Tier I) on Broadband Access Communications, and a Bell Canada/NSERC Industrial Research Chair on Performance & Resource Management in Broadband xDSL Access Networks.

Tad Matsumoto (Fellow IEEE) received his B.S., M.S., and Ph.D. degrees from Keio University, Yokohama, Japan, in 1978, 1980, and 1991, respectively, all in electrical engineering. He joined Nippon Telegraph and Telephone Corporation (NTT) in April 1980. Since he engaged in NTT, he was involved in a lot of research and development projects, all for mobile wireless communications systems. In July 1992, he transferred to NTT DoCoMo, where he researched Code-Division Multiple-Access techniques for Mobile Communication Systems. In April 1994, he transferred to NTT America, where he served as a Senior Technical Advisor of a joint project between NTT and NEXTEL Communications. In March 1996, he returned to NTT DoCoMo, where he served as a Head of the Radio Signal Processing Laboratory until August of 2001; He worked on adaptive signal processing, multiple-input multiple-output turbo signal detection, interference cancellation, and space-time coding techniques for broadband mobile communications. In March 2002, he moved to University of Oulu, Finland, where he served as a Professor at Centre for Wireless Communications. In 2006, he served as a Visiting Professor at Ilmenau University of Technology, Ilmenau, Germany, funded by the German MERCATOR Visiting Professorship Program. Since April 2007, he has been serving as a Professor at Japan Advanced Institute of Science and Technology (JAIST), Japan, while also keeping the position at University of Oulu. Prof. Matsumoto has been appointed as a Finland Distinguished Professor for a period from January 2008 to December 2012, funded by the Finnish National Technology Agency (Tekes) and Finnish Academy, under which he preserves the rights to participate in and apply to European and Finnish national projects. Prof. Matsumoto is a recipient of IEEE VTS Outstanding Service Award (2001), Nokia Foundation Visiting Fellow Scholarship Award (2002), IEEE Japan Council Award for Distinguished Service to the Society (2006), IEEE Vehicular Technology Society James R. Evans Avant Garde Award (2006), and Thuringen State Research Award for Advanced Applied Science (2006), 2007 Best Paper Award of Institute of Electrical, Communication, and Information Engineers of Japan (2008), and Telecom System Technology Award by the Telecommunications Advancement Foundation (2009).

Ha H. Nguyen (M'01, SM'05) received the B. Eng degree from Hanoi University of Technology, Hanoi, Vietnam, in 1995, the M. Eng degree from Asian Institute of Technology, Bangkok, Thailand, in 1997, and the Ph.D. degree from the University of Manitoba, Winnipeg, Canada, in 2001, all in electrical engineering. Dr. Nguyen joined the Department of Electrical Engineering, University of Saskatchewan, Canada in 2001 and is currently a Full Professor. He holds adjunct appointments at the Department of Electrical and Computer Engineering, University of Manitoba, Winnipeg, MB, Canada, and TRLabs, Saskatoon, SK, Canada and was a Senior Visiting Fellow in the School of Electrical Engineering and Telecommunications, University of New South Wales, Sydney, Australia during October 2007-June 2008. His research interests include digital communications, spread spectrum systems and error-control coding. Dr. Nguyen currently serves as an Associate Editor for the IEEE TRANSACTIONS ON WIRELESS COMMUNICATIONS and the IEEE TRANSACTIONS ON VEHICULAR TECHNOLOGY. He is a coauthor, with Ed Shwedyk, of the textbook *A First Course in Digital Communications* (published by Cambridge University Press). He is a Registered Member of the Association of Professional Engineers and Geoscientists of Saskatchewan (APEGS).